Ecological Indicators 135 (2022) 108547

Contents lists available at ScienceDirect

Ecological Indicators

journal homepage: www.elsevier.com/locate/ecolind

Original Articles

Rapid expansion of an aquatic invasive species (AIS) in Central-European surface waters; a case study of *Achnanthidium delmontii*

K. Buczkó [a,b], Zs. Trábert [a], Cs. Stenger-Kovács [c], K. Tapolczai [c,d], T. Bíró [h], M. Duleba [a], A. Földi [a], J. Korponai [a,e,f], E. Vadkerti [e], Zs. Végvári [a,g], É. Ács [a,e,*]

[a] Centre for Ecological Research, Institute of Aquatic Ecology, Karolina út 29, Budapest H-1113, Hungary
[b] Hungarian Natural History Museum, Department of Botany, Könyves Kálmán krt. 40., Budapest H-1087, Hungary
[c] University of Pannonia, Center For Natural Science, Research Group of Limnology, Egyetem u. 10, Veszprém H-8200, Hungary
[d] Balaton Limnological Research Institute, Eötvös Loránd Research Network (ELKH), Klebelsberg Kuno u. 3, Tihany H- 8237, Hungary
[e] University of Public Service, Faculty of Water Sciences, Department of Water Supply and Sewerage, Bajcsy-Zsilinszky utca 12-14, Baja H-6500, Hungary
[f] Department of Environmental Sciences, Sapientia Hungarian University of Transylvania, 400193 Cluj-Napoca, Calea Turzii str. 4, Romania
[g] Senckenberg Deutsches Entomologisches Institut, Eberswalder Straße 90, Müncheberg 15374, Germany
[h] University of Public Service, Faculty of Water Sciences, Department of Regional Water Management, Bajcsy-Zsilinszky utca 12-14, Baja H-6500, Hungary

A R T I C L E I N F O

Keywords:
Site-specific Biological Contamination (SBC) index
Diatoms
River Danube
Water quality
Achnanthidium delmontii
Aquatic invasive species (AIS)

A B S T R A C T

In this work the rapid expansion of a small-celled (<15 μm) monoraphid aquatic invasive species (AIS) along the Central European lotic systems is reported, using the integrated dataset of two large-scale monitoring programs, as supplemented by additional records. *Achnanthidium delmontii* Pérès, Le Cohu & Barthès 2012 (ADMO) was discovered in 2007 and formally described in 2012, on the basis of specimens from a French river. ADMO was first detected in the upper sections of River Danube in 2013, and has been detectable since 2013, and from 2015 onwards in Hungary. The abundance and the number of occupied habitat types by the species have gradually increased. In 2019, ADMO was found to be among the most abundant and the most frequent species in the River Danube, with a mean relative abundance of at least 5%, and a frequency of at least 10% in samples. To extend the Danubian dataset, the relative abundances of ADMO from 79 freshwater lotic samples were studied to assess their potential of the species as an indicator organism. Weighted average regression was employed to determine the species' optima and tolerances for 18 environmental variables. ADMO has a wide ecological range, which serves to confirm its potential invasive behaviour. In the case of the following variables, the values were found to be consistent with previously published data on the requirements of the taxon. Despite ADMO prefers high temperatures (estimated optimum = 21.8 °C), its spread shows a downstream pattern of the main watercourses of Europe. The species was first found abundantly from the upper section of River Danube, then with increasing abundance in the middle section, while remaining rare in the lower section. This distribution demonstrates that the River Danube serves as an important linear route for the species' invasion.

The results of the study will help improve the ecological classification of water bodies and inform water protection actions undertaken under the auspices of the Water Framework Directive (WFD).

1. Introduction

Aquatic photoautotrophs are in the basis of the food web, and as such, any change in the quantity and community composition of them can result in a cascade effect in waterbodies. Aquatic invasive species (AIS) are particularly pervasive, and may cause food web disruption, water quality deterioration and local species extinctions (Macêdo et al., 2021). The loss of taxa and the destruction of the integrity of the systems together pave the way for the emergence of new taxa. Indeed, AIS are able to establish their presence rapidly, proliferate and modify or completely reorganize communities. In spite of all this, the biogeography of invasive microorganisms is a neglected field of research. This is mainly due to difficulties in sampling, inefficient detection strategies and outstanding problems in their taxonomy (Crossetti et al., 2019; Macêdo et al., 2021; Moreira et al., 2015).

Diatoms are useful indicators of several environmental changes, such

* Corresponding author at: Centre for Ecological Research, Institute of Aquatic Ecology, Karolina út 29, Budapest H-1113, Hungary.
E-mail address: acs.eva@uni-nke.hu (É. Ács).

https://doi.org/10.1016/j.ecolind.2022.108547
Received 23 August 2021; Received in revised form 3 January 2022; Accepted 5 January 2022
Available online 10 January 2022

as acidification, nutrient enrichment, and changes in the variability in water temperature and conductivity (Rimet and Bouchez, 2012). Furthermore, benthic littoral diatoms are considered powerful indicators of local pollution sources and diatom-based indices are among the first predictive tools capable of detecting the deterioration of freshwater environments (Rimet et al., 2016). As long ago as 2000, the criteria of invasive diatom species were defined according to their i) recent appearance; ii) absence from the usual flora; iii) proliferation; iv) rapid expansion (Coste and Ector, 2000). Over the past decade or so, an increasing number of research projects with a focus on the invading phenomenon of diatoms have been published, among them, several in connection with global climate change (Duleba et al., 2014; Falasco et al., 2016; Spaulding et al., 2010). Most of them focused on the *Didymosphenia geminata* (Lyngbye) Mart.Schmidt 1899*,* a diatom species which gained a name for itself through its negative effects on stream habitats and food resources of fish, and was considered a nuisance with an adverse effect on recreational activities through its causing a number of cases of serious water quality deterioration (Blanco and Ector, 2009; Bray et al., 2016; Jellyman et al., 2011; Mather et al., 2010; Sastre et al., 2013). Some *Achnanthidium* species also have an invading strategy, meeting the criteria of an AIS (Falasco et al., 2016; Pérès et al., 2012; Plamen, 2018; Rimet et al., 2010). Species belonging to this genus are common diatoms, often dominant in biofilms.

Recently, compositional changes of the benthic diatom assemblages caused by an achnanthoid taxa along the River Danube have been detected – and this is but an instance of a wider phenomenon in which remarkable changes in riverine diatom assemblages is to be witnessed thanks to the rapid spread of *Achnanthidium delmontii* Pérès, Le Cohu & Barthès 2012 (ADMO). ADMO was originally described in the Vieux Rhin in France in 2007 (Pérès et al., 2012). Following this, parallel increases in relative abundances were documented in a Mediterranean river (the River Cèze) from 2008 to 2010, from the Rhône in 2009 and 2010, and ADMO's consistent presence was reported in Italy from 2014 (Falasco et al., 2016). Next in chronological order, is France in 2016 (Keck et al., 2018; Peeters and Ector 2018), then in 2018, ADMO was reported in the Hungarian section of Danube. In 2019 ADMO was found in 26 samples (of which were in 10 in Hungary) along the whole River Danube. Furthermore, ADMO had reached the Soroksári-Danube Arm, indicating its inrush into the tributaries of the river (Fidlerová and Makovinská, 2021).

It is worth noting that the first report of ADMO in North America exactly coincided with its first occurrence in Europe, both being in 2007. ADMO seems to be expanding throughout the eastern US (Ciugulea and Potapova, 2021).

Because the exact identification challenges the beginner analysts, and in some samples the monoraphid ADMO can be rare and sporadic, in this study we aim to (1) providing a detailed taxonomic description to support its accurate identification; (2) analyzing the appearance and the spread of the ADMO in the River Danube and its tributaries; (3) using weighted average analysis, calculating its optima and tolerance values for 18 environmental variables to characterize its autecological features, additionally presenting associated taxa; (4) applying the Site-specific Biological Contamination (SBC) invasion index, and assessing the risk of the appearance and proliferation of ADMO and other invasive species, and analyzing the impact of ADMO on diatom community.

2. Material and methods

An "ADMO" database was built using the results of the microscopic analysis of 142 phytobenthos samples with the aim of studying the distribution of ADMO and its effects on the structure of the diatom community (Table 1). Samples were collected between 2013 and 2020 from (1) sites of the 3rd and 4th Joint Danube Surveys (JDS3 and 4), from 2013 and 2019 (from the upper and middle sections of the Danube in Hungary down to the southern border (Fig. 3, Liška et al., 2021), and (2) the whole Hungarian section of the River Danube (Fig. 4, Trábert et al., 2020), and (3) within the national survey in Hungary between 2018 and 2019.

Table 1
Overview of the database and dataset used to study the effect of *Achnanthidium delmontii* (ADMO) on the diatom assemblages in this research.

	Dataset	Description of dataset	Number of items
I.	ADMO database	all phytobenthos samples in this study	n = 142
IIA	$ADMO_{\mathbf{Dd}}$	Danube dataset	n = 128
IIB	$ADMO_{\mathbf{IN}}$	Samples, in which ADMO was recorded	n = 79
IIA-1	$ADMO_{Dd\_\mathbf{in}}$	Within $ADMO_{Dd}$ dataset where ADMO was present	n = 65
IIA-2	$ADMO_{Dd\_\mathbf{np}}$	Within $ADMO_{Dd}$ dataset where ADMO was not present	n = 63
IIA-1+	${ADMO_{Dd\_in}}^{+}$	Identical with $ADMO_{Dd\_in}$ dataset ADMO was present	n = 65
IIA-1-	${ADMO_{Dd\_in}}^{-}$	ADMO was removed from ${ADMO_{Dd\_in}}^{+}$	n = 65
IIB+	${ADMO_{IN}}^{+}$	${ADMO_{IN}}^{+}$ identical with $ADMO_{\mathbf{IN}}$	n = 79
IIB-	${ADMO_{IN}}^{-}$	ADMO was removed from ${ADMO_{IN}}^{+}$	n = 79
IIB + 5	${ADMO_{IN}}^{+\geq 5\%}$	${ADMO_{IN}}^{+}$ group was divided into two subgroups based on relative abundance of ADMO. ${ADMO_{IN}}^{+\geq 5\%}$ where ADMO is dominant	n = 20
IIB	${ADMO_{IN}}^{+<5\%}$	${ADMO_{IN}}^{+}$ group was divided into two subgroups based on relative abundance of ADMO. ${ADMO_{IN}}^{+<5\%}$ where ADMO is not dominant	n = 59
IIB	${ADMO_{IN}}^{-\geq 5\%}$	ADMO was removed from ${ADMO_{IN}}^{+\geq 5\%}$	n = 20
IIB	${ADMO_{IN}}^{-<5\%}$	ADMO was removed from ${ADMO_{IN}}^{+<5\%}$	n = 59

In the database, ADMO 79 samples were recorded: 65 from the Danube, and 14 from its tributaries in Hungary ($ADMO_{\mathbf{IN}}$ dataset).

From the initial dataset, 128 diatom samples were selected, their selection being restricted to those from the Danube (**D**anubian **d**ataset = **Dd**) (Table 1). In the $ADMO_{\mathbf{Dd}}$ dataset, ADMO was detected in 65 samples (designated $ADMO_{\mathbf{Dd\_in}}$,), while in 63 samples no ADMO was present (designated $ADMO_{\mathbf{Dd\_np}}$). The idea here was to create two balanced groups of sites to fulfil the mathematical criteria of the statistical tests to be carried out.

In order to discover the effect of ADMO on the diatom community structure, ADMO was retained in (${ADMO_{Dd\_in}}^{+}$ [n = 65]) and removed from (${ADMO_{Dd\_in}}^{-}$ [n = 65]), the dataset of the $ADMO_{Dd\_in}$. Additional datasets were created ${ADMO_{Dd\_in}}^{-}$ [n = 65], ${ADMO_{IN}}^{-}$ [n = 79] by removing ADMO from the $ADMO_{Dd\_in}$ and $ADMO_{IN}$ datasets, respectively.

As a next step, the $ADMO_{IN}$ group was divided into two subgroups, based on the relative abundance of ADMO. Sites where the relative abundance of ADMO was ≥5% (ADMO is dominant) were designated ${ADMO_{IN}}^{+\geq 5\%}$ (n = 20). The subgroup ${ADMO_{IN}}^{+<5\%}$ (n = 59) contains the rest of the samples in which ADMO's relative abundance was <5%. After retaining and removing ADMO, the subgroups ${ADMO_{IN}}^{-\geq 5\%}$ (n = 20) and ${ADMO_{IN}}^{+\geq 5\%}$ (n = 20) were obtained. Similarly, ${ADMO_{IN}}^{-\leq 5\%}$ (n = 59) was created by the removal of ADMO from the ${ADMO_{IN}}^{+<5\%}$ (n = 59) dataset.

2.1. Environmental variables

Phytobenthos and water samples were collected in parallel. Temperature, conductivity, pH, dissolved oxygen and turbidity were measured in the field using a portable Hanna Multi Meter (Hanna Instrument, Woonsocket, RI, USA) and a turbidity meter (Lovibond, Dortmund, Germany), respectively. In the laboratory, total phosphorous (TP) and nitrite (${NO_2}^{-}$) concentrations were determined using standard titrimetric and spectrophotometrical methods. Anion (Cl^{-}, ${SO_4}^{2-}$, ${NO_3}^{-}$, ${HCO_3}^{-}$, ${PO_4}^{3-}$) and cation (Na^{+}, K^{+}, Mg^{2+}, Ca^{2+}) concentrations were measured via DIONEX dual channel ion chromatography (Thermo

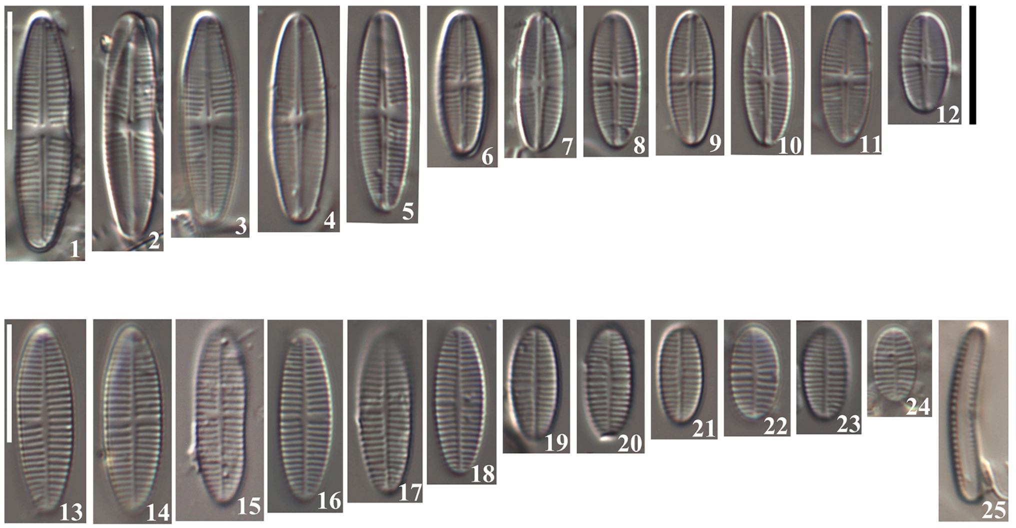

Fig. 1. Light microscopic (LM) photos of ADMO. Fig. 1: 1–25. *Achnanthidium delmontii* Pérès, Le Cohu & Barthès 2012. LM: (1, 3, 7) raphe valves, (24) rapheless valve and (25) girdle view from Dráva-alsó (at Barcs); (2, 4–6, 8–12) raphe valves and (13–23) rapheless valves from the River Danube (at Gönyű, from the left bank of the river). Scale bar 10 µm.

Fisher Scientific, Waltham, MA, USA). Total organic carbon and total nitrogen concentrations were determined using a Multi N/C 3100 TC-TN analyzer (Analytik Jena, Jena, Germany).

2.2. Diatom sample processing

Phytobenthos samples were collected according to the standard methods (CEN, 2014); they were preserved in formaldehyde (4% final concentration) until preparation. Diatom frustules were cleaned with hydrogen peroxide and hydrochloric acid, permanent slides were mounted using Naphrax (refractive index: 1.74), (CEN, 2014). Diatom valves were counted under an Olympus IX70 inverted microscope equipped with differential interference contrast (DIC) optics, at a magnification of 1500×. A minimum of 400 valves was identified to species or genus level in every samples. SEM images were created using a Zeiss EVO MA 10 scanning electron microscope (SEM). For SEM preparations, a part of the cleaned and washed samples was filtered through a 3 µm Isopore™ polycarbonate membrane filter (Merck Millipore), which was fixed onto a stub using double-sided carbon tape and coated with gold using a rotary-pumped spatter coater (Quorum Q150R S) and observed at 10 kV with an 8-mm working distance, using a secondary electron detector in high vacuum mode.

Metabarcoding data of phytobenthos samples: Additionally, data based on the results of the metabarcoding survey of JDS4 were used to confirm the identification of ADMO and its distribution in the River Danube (Zimmermann et al., 2021). Atogether 69 bulk DNA metabarcoding samples were collected, and two molecular markers were amplified using a polymerase chain reaction (PCR), the nuclear-encoded V4 region of the 18S rRNA gene according to (Visco et al., 2015) and a fragment of the plastid *rbc*L gene according to (Vasselon et al., 2017). ADMO could be detected solely by the latter marker, thus only the results of the examination of the *rbc*L marker are presented here. Sequences were taxonomically assigned to ADMO using the Diat.barcode (version 9) reference barcode library for diatoms (Rimet et al. 2019).

In order to estimate the degree of biocontamination, the Site-specific Biological Contamination (SBC) index was also calculated (Liška et al., 2008), as formulated in Csányi et al. (2021).

$$\mathrm{SBC} = (n_a/n_{sum} + log N_a/log N_{sum})/2,$$

where n_a is the number of alien species, n_{sum} the number of all species in the sample, N_a the abundance of alien species and N_{sum} the total abundance of species in the sample. The SBC index involves both the specific value of number of alien species and the specific value of an abundance of alien species in the total community (Arbačiauskas et al., 2008; Paunović et al., 2015). The value of the SBC index can vary between 0 (no biocontamination) and 1 (maximal biocontamination). SBC index was calculated with and without ADMO. This index is widely applied metrics for macrozoobenthos and fish communities (Liska et al., 2021).

The following diatom taxa were considered AIS: *Achnanthidium catenatum* (Bily & Marvan) Lange-Bertalot 1999*, A. delmontii, A. druartii* Rimet & Couté 2010*, A. rivulare* Potapova & Ponader 2004*, A. subhudsonis* (Hustedt) H.Kobayasi 2006*, Diadesmis confervacea* Kützing 1844*, Reimeria uniseriata* S.E.Sala, J.M.Guerrero & M.E.Ferrario 1993 (Coste and Ector, 2000; Lange-Bertalot et al., 2017, Ector et al., 2017).

2.3. Statistical analysis

Weighted average regression was employed in an attempt to infer the ADMO optimum values (opt) and tolerance (tol) to 18 environmental variables. The degree of homogeneity of group dispersion was tested using the "betadisper" function available in the "vegan" package (Oksanen et al., 2007) in the R statistical programming environment (R Core Team, 2020).

Differences in the community composition of the separated groups were explored using non-parametric multi-variate statistical methods (NMDS) (Clarke, 1993), based on Euclidian distance. NMDS seeks an ordination in which the distances between all pairs of samples are in rank order agreement with their degree of dissimilarity in species composition (Borcard et al., 2018; Ludwig and Reynolds, 1988). Two NMDS axes were calculated, and PERMANOVA was used on the NMDS scores to test if the scores of calculated NMDS axes is differentiated. Hellinger-transformed relative abundance was calculated first on the $\mathrm{ADMO_{Dd}}$ dataset:

(1) This method was used first to compare on the $\mathrm{ADMO_{Dd\_in}}$ and $\mathrm{ADMO_{Dd\_np}}$ groups. PERMANOVA ("adonis" in the "vegan" package) was employed on NMDS components to test the overall effect of ADMO on ordination. PERMANOVA is largely unaffected by heterogeneity for balanced design (Anderson and Walsh, 2013; Anderson and Walsh, 2013).
(2) The analysis described in (1) was repeated on the $\mathrm{ADMO_{Dd\_in}}^{-}$, $\mathrm{ADMO_{Dd\_np}}$ (3) $\mathrm{ADMO_{IN}}^{+\geq5\%}$, $\mathrm{ADMO_{IN}}^{+<5\%}$ (4) $\mathrm{ADMO_{IN}}^{-\geq5\%}$ $\mathrm{ADMO_{IN}}^{-<5\%}$ datasets.

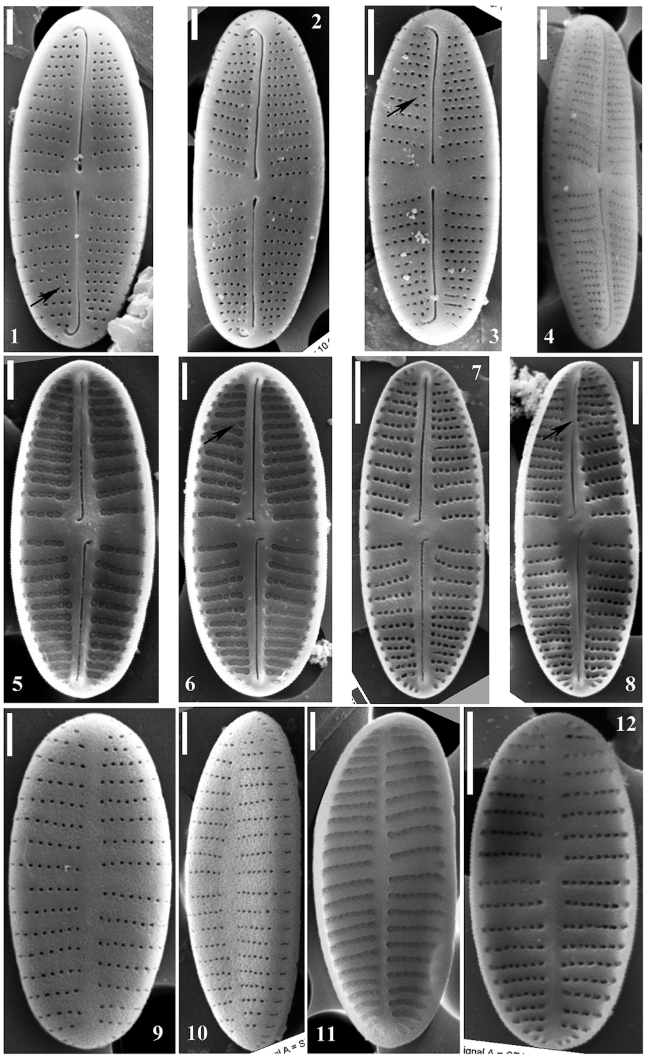

Fig. 2. Scanning electron microscopic (SEM) photos of ADMO. Fig. 2: 1–12. *Achnanthidium delmontii* Pérès, Le Cohu & Barthès 2012. SEM: (1–3) external view of the raphe valve; (4) external girdle view of the raphe valve showing interruption between the valve face striae and the mantle areolae; (1, 3) external view of the raphe valve showing a Voigt fault (indicated by arrows); (5–8) internal view of the raphe valve; (6, 8) internal view of the raphe valve showing a Voigt fault (see the arrows); (9) external view of the rapheless valve showing interruption in the row of mantle areolae at the apices; (10) external girdle view of the rapheless valve showing interruption between the valve face striae and the mantle areolae; (11, 12) internal view of the rapheless valve. Scale bars 1 μm (1, 2, 5, 6, 9, 11) and 2 μm (3, 4, 7, 8, 10, 12).

The resulting NMDS plots were then compared using Procrustes analysis with a permutation test (Gower, 1971; Peres-Neto and Jackson, 2001).

Procrustes analysis was used to investigate the degree of concordance between each pair of ordinations. Procrustes analysis rotates two ordinations to maximize the similarities between them by minimizing the sum of their squared distances (Gower, 1971). The residuals of a Procrustes rotation reflect the extent of the changes in the position of assemblages in the NMDS space. Residuals are high if the removal of ADMO strongly modifies the structure of the assemblages. The Procrustes rotation was computed by means of the "procrustes" function in the vegan package (Oksanen et al., 2013).

3. Results

Altogether 513 taxa were distinguished in the dataset representing 142 phytobenthos samples. In the $ADMO_{Dd\_in}$ dataset, 429 taxa could be identified from among the 65 samples, the average taxonomical richness (average of number of taxa) of which was 46; whereas the average number of taxa was 40.2 among the 63 samples of $ADMO_{Dd\_np}$.

3.1. Morphology of Achnanthidium delmontii

The valves are linear with rounded apices, becoming elliptical in small individuals (Fig. 1). On the raphe valve, the axial area is narrow, the central area irregular, and in general, forms a rectangular fascia, often with one shortened stria on one of the margin sides. The filiform, straight raphe has distinct central pores; striae are barely radial. On the rapheless valve, the axial area is acicular, and striae are parallel, and slightly radiate towards the apices. Two striae are slightly more spaced in the middle part of the valve. In the girdle view, the frustules are slightly bent, and striae are clearly visible. In this study, the lengths of the valves are 7–20 μm (mean = 12.6 ± 3.7), and the widths 4–5 μm (mean = 4.4 ± 0.3). On the raphe valves, the number of stria is 21–26 (mean = 23.7 ± 1.3) in 10 μm, and 18–22 in 10 μm (mean = 24.3 ± 0.7) on rapheless valves.

When examined using a scanning electron microscope, it becomes apparent that the external valve has straight raphe with droplet-like proximal endings (Fig. 2). The terminal fissures are deflected to the same side and terminate on the valve face near the valve margin. In some cases, the Voigt fault can be detected as a shortened stria. Internally, the proximal raphe endings are bent in the opposite direction. The distal raphe endings terminate in helictoglossae. On the raphe valve, the striae are composed of 5 to 7 almost rounded areolae. On the rapheless valve, the striae consist of 6 to 7 areolae, and two of them are more distant, in the middle part of the valve. On both valves, the areolae are internally occluded by hymens, and rimmed by fine slits. There is a row of elongated areolae on the mantle. The mantle row of striae on rapheless valves is interrupted at the apices.

3.2. Occurrence and spread of ADMO in the River Danube and its watercourses

2013 was the first year in which ADMO were recorded, albeit in low abundances (<3%), in the dataset of ten sites in the German and Austrian sections of the River Danube. Three years later (2016) ADMO was sporadically detected, as a rare taxon along the Hungarian section of the river downstream. It is worth noting that, it was present at Paks, close to the cooling water inflow of the Paks Nuclear Power Plant, where the temperature of the water is usually elevated. ADMO had high frequency but low abundance (relative abundance was <2%) in all Hungarian samples in 2016. By 2018, however, ADMO was found at more than 85% of the Hungarian sampling points in the River Danube (n = 28). Moreover, in 40% of these samples, ADMO was already a dominant species (more than 5% in relative abundance and reaching a relative abundance of 65%). The number of records of ADMO has been steadily increasing in 2019; thus, it has become an abundant and frequent member of the diatom assemblages of the Danubian phytobenthos (Fig. 3).

In 2020, ADMO's relative abundance reached more than 90% in the warm water effluents from the power station at Paks. Moving away from the River Danube, in 2019 and 2020 ADMO was recorded in 14 surface running waters in Hungary, and in two of them it was dominant (>5%) in relative abundance (Fig. 4).

Comparing the result of an analysis of the morphology-based occurrences of ADMO (Fig. 3 upper panel) with the data come from the metabarcoding analysis (Fig. 3 lower panel), the match is obvious. Based on the 66 samples from 2019 which were analysed with both microscopy and metabarcoding, ADMO was detected with both methods in 25 (37.9%) samples and was absent in 11 (16.7%) samples. It was detected

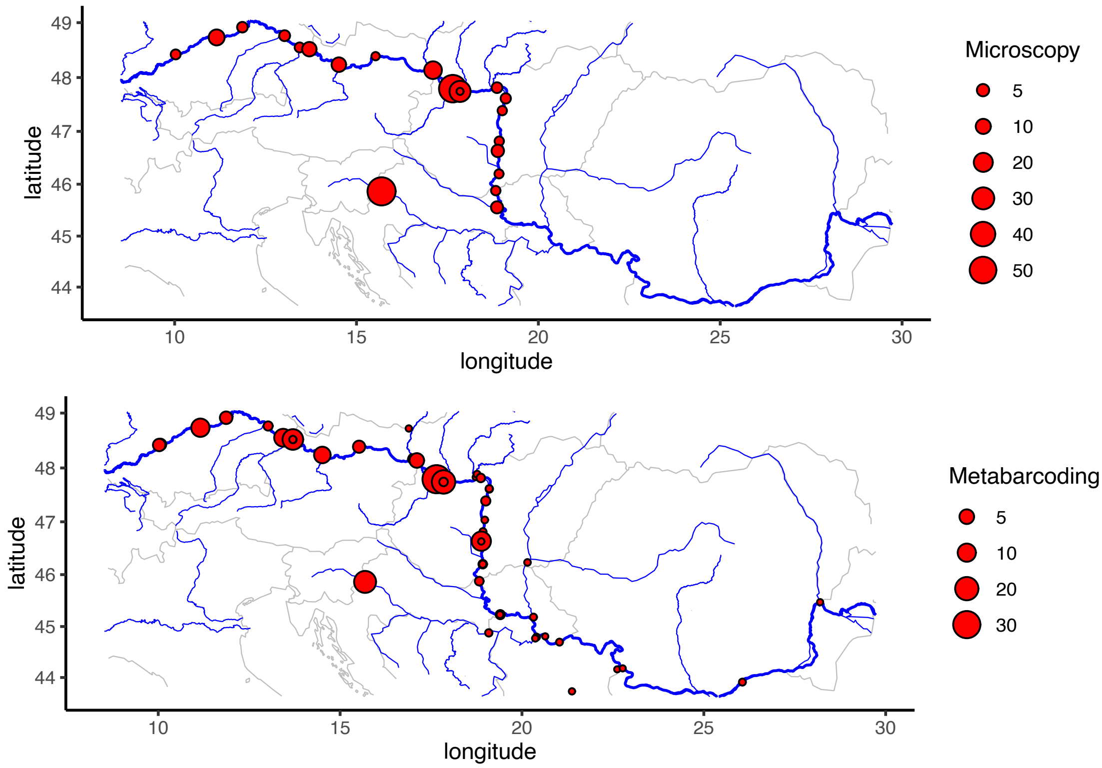

Fig. 3. Relative abundance (%) of *Achnanthidium delmontii*, in the River Danube based on morphological (microscopical) analysis (upper panel) and metabarcoding analysis (lower panel). (Data derived from the Joint Danube Survey (2019) (Liška et al., 2021; Zimmermann et al., 2021).

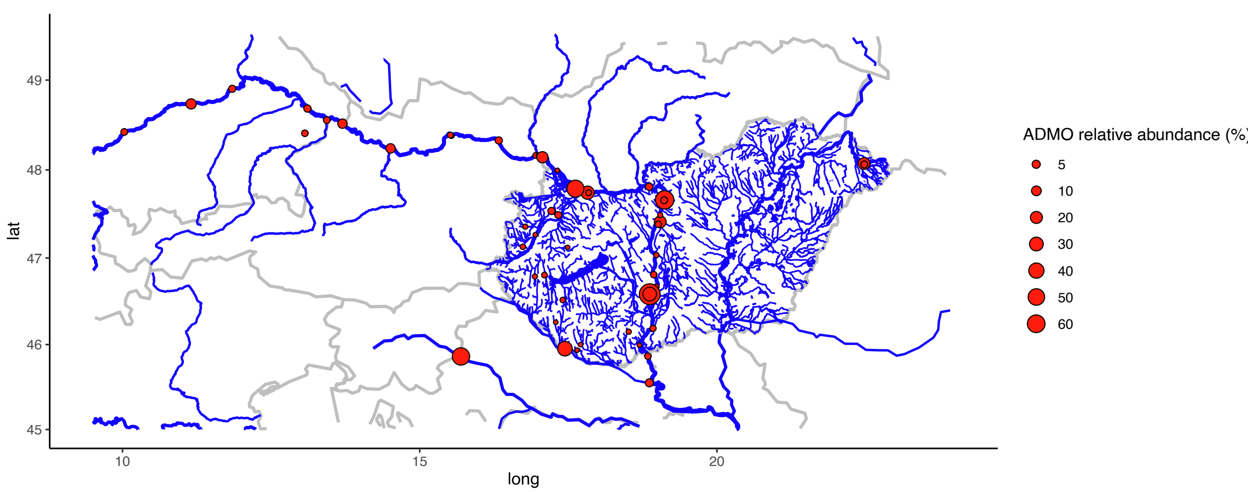

Fig. 4. Distribution map of *Achnanthidium delmontii* in Hungary and the upper section of River Danube between 2013 and 2020. Data illustrated here are based on morphology.

only by metabarcoding in 30 (45.5%) samples, and there was not one sample where it was observed only with microscopy. The relative abundance of ADMO detected with the two methods correlated significantly (Pearson's r = 0.87, $p < 0.01$). The morphology-based microscopic observation received strong validation from the molecular results in 2019.

The metabarcoding method resulted in a high-resolution snapshot describing the distribution of ADMO along the River Danube and its tributaries, based on the data of a two week long sampling campaign in 2019 (Liška et al., 2021). As illustrated in Fig. 3, according to the *rbc*L-based evidence, ADMO was among the most abundant diatoms in the River Danube, as well as in the tributaries of the river (Liška et al., 2021; Zimmermann et al., 2021).

3.3. Autecological preferences and associated taxa of ADMO

Table 2 on the basis of its autecological preferences, ADMO can be regarded as an alkaliphilic (pH opt = 7.8, tol = 0.2) diatom that prefers higher temperatures (opt = 21.8 °C, tol = 2.2 °C), low conductivity (opt = 318 μS cm^{-1}, tol = 48 μS cm^{-1}) and elevated nutrient concentration: (TP (opt = 129 μg L^{-1}, tol = 47 μg L^{-1}), TN (opt = 1.5 mg L^{-1}, tol = 0.6 mg L^{-1}).

When ADMO reached a relative abundance of 60% the accompanying dominant taxa were *Achnanthidium druartii*, *Achnanthidium lineare*

Table 2
Achnanthidium delmontii optimum and tolerance for 18 environmental variables. (n = number of samples).

	Optimum	Tolerance	n	Dataset
T (°C)	21.8	2.2	54	$ADMO_{IN}$
pH	7.8	0.2	58	$ADMO_{IN}$
conductivity(μScm^{-1})	318	48	58	$ADMO_{IN}$
DO (mgl^{-1})	8.5	0.9	31	$ADMO_{Dd\_in}$
SS (mgl^{-1})	32.7	14.6	31	$ADMO_{Dd\_in}$
TP (μgl^{-1})	129	47	58	$ADMO_{IN}$
PO_4^{3-} (μgl^{-1})	55.5	49.2	44	$ADMO_{IN}$
TN (mgl^{-1})	1.5	0.6	54	$ADMO_{IN}$
NO_3^- (mgl^{-1})	5.0	2.0	48	$ADMO_{IN}$
NO_2^- (mgl^{-1})	0.02	0.04	48	$ADMO_{IN}$
TOC (mgl^{-1})	2.2	0.8	36	$ADMO_{Dd\_in}$
Ca^{2+} (mgl^{-1})	51.5	8.4	49	$ADMO_{IN}$
Mg^{2+} (mgl^{-1})	30.2	4.5	49	$ADMO_{IN}$
Na^+ (mgl^{-1})	13.5	3.5	35	$ADMO_{Dd\_in}$
K^+ (mgl^{-1})	4.7	0.4	35	$ADMO_{Dd\_in}$
HCO_3^- (mgl^{-1})	165	33	39	$ADMO_{Dd\_in}$
SO_4^{2-} (mgl^{-1})	26.3	5.5	39	$ADMO_{Dd\_in}$
Cl^- (mgl^{-1})	16.1	5.4	39	$ADMO_{Dd\_in}$

(W. Smith) 1855, *Achnanthidium rivulare*, *Amphora pediculus* (Kützing) Grunow 1875 and *Cocconeis euglypta* Ehrenberg 1854.

3.4. SBC index and the impact of ADMO on the diatom community

The Site-specific Biological Contamination (SBC) index values in the $ADMO_{IN}$ dataset are presented in the order of increasing relative abundance of ADMO in Fig. 5. The value of SBC varied between 0.01 and 0.62, (mean = 0.25 ± 0.14, n = 79). Low SBC values (<0.02) were calculated for brooks, where *Achnanthidium minutissimum* (Kützing) Czarnecki 1994, *A. pyrenaicum* (Hustedt) H.Kobayasi 1997*, Amphora pediculus,* and *Craticula subminuscula* (Manguin) C.E.Wetzel & Ector 2015 were the dominant associated taxa. The SBC index reached its highest value in the River Danube at Paks, with 73% of ADMO where *Achnanthidium druartii, A. eutrophilum* (Lange-Bertalot) Lange-Bertalot 1999*, A. rivulare, A. minutissimum* and *Amphora pediculus* were the associated taxa. Overall, SBC values varied broadly across the 79 samples.

SBC index was also calculated without ADMO. There were 27 samples in $ADMO_{IN}$ dataset that ADMO was the only AIS; and in the rest of 52 samples other invader diatoms were detected. The value of SBC without ADMO in these 52 samples varied between 0.01 and 0.52, (mean = 0.15 ± 0.12, n = 52).

The SBC index values in the function of logarithmic relative abundance of ADMO are presented on Fig. 6. The increasing abundance of ADMO has a significant, positive correlation with SBC values calculated with and without ADMO; $R^2 = 0.84$, $p < 0.001$ and $R^2 = 0.11$, $p < 0.01$ respectively.

3.4.1. Community composition of Danubian samples ($ADMO_{Db}$)

Group dispersions of the Hellinger transformed data were homogenous (betadisper, F = 2.6289, permutation = 999, p = 0.102) for the $ADMO_{Dd\_in}$ data matrix, as well as in the $ADMO_{Dd\_np}$ data matrix (betadisper, F = 2.1852, permutation = 999, p = 0.128). ADMO is influential in structuring the phytobenthos communities in both data matrices $ADMO_{Dd\_in}^+$ (adonis, F = 6.424, $R^2 = 0.046$, p = 0.001) and $ADMO_{Dd\_in}^-$ (adonis, F = 4.008, $R^2 = 0.031$, p = 0.001).

A strong overlap may be observed between the groups $ADMO_{Dd\_in}$ and $ADMO_{Dd\_np}$ on the NMDS plot (Fig. 7/a), but different composition patterns are seen in both the $ADMO_{Dd\_in}^+$ and $ADMO_{Dd\_in}^-$ matrices (Fig. 7/b) in terms of the NMDS scores ($ADMO_{Dd\_in}^+$: adonis: F = 12.934, R^2 = 0.0931, p = 0.001; $ADMO_{Dd\_in}^-$: F = 4.4881, R^2 = 0.03439, p = 0.015), suggesting that the differentiation is quite much stronger when ADMO is in.

3.4.2. Procrustes of $ADMO_{Db}$ sites

A significant degree of correlation between the two ordinations was found (correlation = 0.8509, P = 0.001 on 999 permutations; Fig. 7/c). The majority of sampling sites are in the same relative positions, but generally shifted away from the center of the ordination diagram. The increased distances between sampling sites suggests that diatom assemblages become less similar. A direction and difference between the two locations of a site (indicated by a longer arrow) indicate a great effect by ADMO on the community.

3.4.3. Community composition in all occurrences ($ADMO_{IN}$)

Group dispersions of the Hellinger-transformed data in the $ADMO_{IN}^+$ dataset were heterogeneous (betadisper, F = 14.919, permutation = 999, p = 0.002), but homogenous in the $ADMO_{IN}^-$ data matrix (betadisper, F = 2.2818, permutation = 999, p = 0.142). These scores of data analysis seem to indicate that the structure of phytobenthic assemblages is significantly affected by presence of ADMO.

The $ADMO_{IN}^{+\geq 5\%}$ dataset was separated from the others (F =

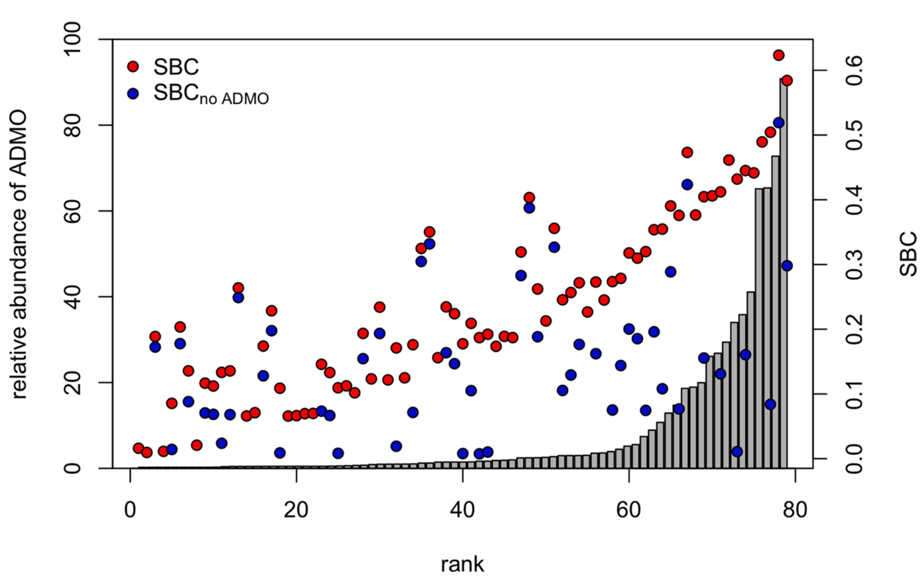

Fig. 5. Site-specific Biological Contamination Index (SBC) values calculated with and without *Achnanthidium delmontii* (ADMO). The samples are arranged in order of the increasing relative abundance of ADMO.

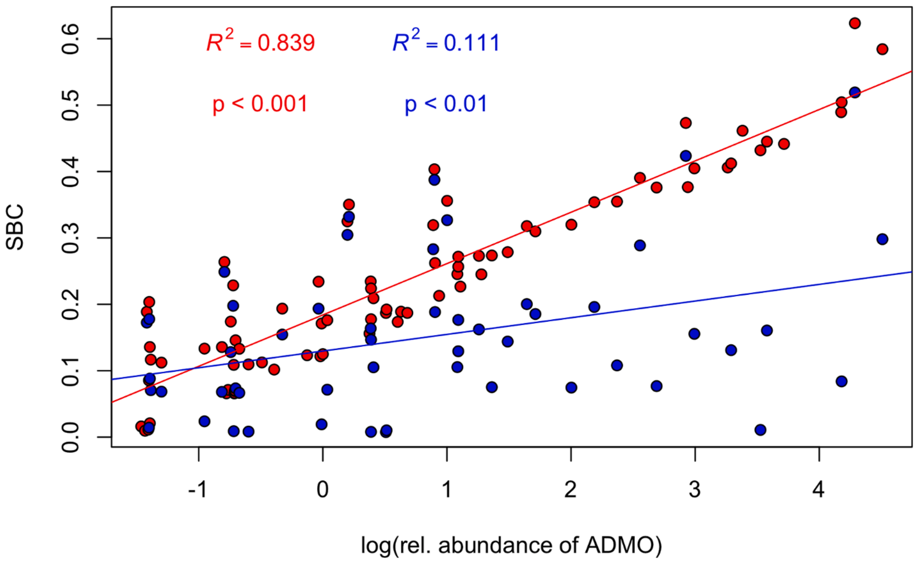

Fig. 6. SBC index values in function of the logarithmic relative abundance of *Achnanthidium delmontii* (ADMO). Red circles represent SBC index calculated on the $ADMO_{IN}$ dataset (n = 79). Blue circle represents the SBC index values calculated after removing ADMO from the dataset (n = 52, in 27 samples ADMO was the only AIS). Red (with ADMO) and blue (without ADMO) solid lines show the associated correlations. (For interpretation of the references to colour in this figure legend, the reader is referred to the web version of this article.)

6.3613, $R^2 = 0.07631$, p = 0.001), and also even when the ADMO were excluded from the data matrix $ADMO_{IN}^{-\geq 5\%}$ (F = 2.3922, $R^2 = 0.03$, p = 0.001).

The results of the NMDS analyses are presented in Fig. 7/d in the case of $ADMO_{IN}^{+\geq 5\%}$ and $ADMO_{IN}^{+<5\%}$. The degree of separation of two groups is significant. There is a weak overlap between the $ADMO_{IN}^{+\geq 5\%}$ and $ADMO_{IN}^{+<5\%}$ samples (adonis: F = 19.439, R^2 = 0.20157, p = 0.001) (Fig. 7/d). The same pattern (i.e. the degree of overlap is small) can be seen in Fig. 7/e on the NMDS plot comparing the $ADMO_{IN}^{-\geq 5\%}$ and $ADMO_{IN}^{-<5\%}$ data matrices in terms of the NMDS scores (F = 8.7012, R^2 = 0.10153, p = 0.002). There is clear visual evidence that diatom assemblages are different in structure in the samples where ADMO is considered a dominant species and in those in which its abundance is less than 5%.

3.4.4. Procrustes of $ADMO_{IN}$ sites

A significant degree of correlation was found between the two ordinations of ADMO $_{IN}^{+}$ and ADMO $_{IN}^{-}$ (correlation = 0.8746, P = 0.001 for 999 permutations; (Fig. 7/f)). Most of the sites are located in the same relative positions, but generally shifted away from the center of the ordination diagram. The increased distances between sampling sites suggests that, diatom assemblages become less similar. A direction and greater difference between the two locations of a site (indicated by a longer arrow) indicate a greater effect by ADMO on the community.

4. Discussion

4.1. Taxonomy

The representatives of the genus *Achnanthidium* show a high degree of morphological variation and phenotypic plasticity, but worldwide they are often numerous, abundant, and frequent contributors to the phytobenthos (Martín et al., 2010; Novais et al., 2015; Miao et al., 2020). The identification of the Achnanthidium taxa is difficult due to their small cell size and the insufficient amount of information available on diatom floras; nonetheless, species-level identification would undoubtedly lead to more accurate bioassessment (Ponader and Potapova, 2007). Recent observations of the *Achnanthidium* taxa also support the idea that the species-level identification and the discovery of new taxa are far from negligible factors in high-quality water bioassessment and management (Miao et al., 2020).

The populations presented in this study display a high level of agreement with the original description of ADMO (Pérès et al., 2012). This species has several features which facilitate its correct identification even in LM, though its monoraphid nature (the two valves of a frustulum differing from each other) can cause some difficulties, especially if the species abundance is low in a sample, and/or the analyst is less experienced in diatom taxonomy. The co-occurrence of morphologically similar achnanthoids can also complicate the counting procedure. Their main characteristic features are the following: (1) outline (the valves being linear with rounded apices, becoming elliptical in small individuals); (2) the axial area is narrow on the raphe valve; (3) the irregular central area generally forms a rectangular fascia often with a shortened stria on one of the margin sides; (4) the filiform, straight raphe has distinct central pores; (5) striae are barely radial; (6) on the rapheless valve the axial area is acicular; (7) on the rapheless valve striae are parallel-to-slightly-radiate at the apices; (8) in most cases, two striae are slightly more spaced apart in the middle part of the valve.

Briefly, ADMO can be safely identified in LM based on outline and the striae pattern of the central area, though checking under an SEM can improve the reliability of identification. Moreover, the recent developments in DNA metabarcoding and high-throughput sequencing (HTS) offer a cost-effective way for the taxonomic assignment of diatoms (Nistal-García et al., 2021; Tapolczai et al., 2021). Relative abundance calculated from the microscopic identification have a slightly higher value than those from metabarcoding. It can be due to the fact that smaller taxa are usually overrepresented in microscopic datasets as their abundance is based on frustule counts, not considering the biomass difference between taxa. In contrast, it is already shown that relative abundance inferred from read numbers in metabarcoding studies of diatoms correlates well with cell biovolume (Vasselon et al., 2018). In the case of such small taxa as ADMO, this difference can be important. However, this effect is supposedly counterbalanced by the higher sensitivity of metabarcoding to detect the species.

This, then means a further base for the discovery of the invasion routes and patterns of invasive algae species in the future, as here, in the case of ADMO.

4.2. Appearance and expansion of ADMO

The River Danube is one of the best studied watercourses of the world, due to the regular national and international monitoring programs, like the Joint Danube Survey. The study of the Danubian phytobenthos started in 1980s in our lab. The same research group examined the composition and structure of biofilm over decades and got a complex overview of it. Moreover, the permanent slides made it

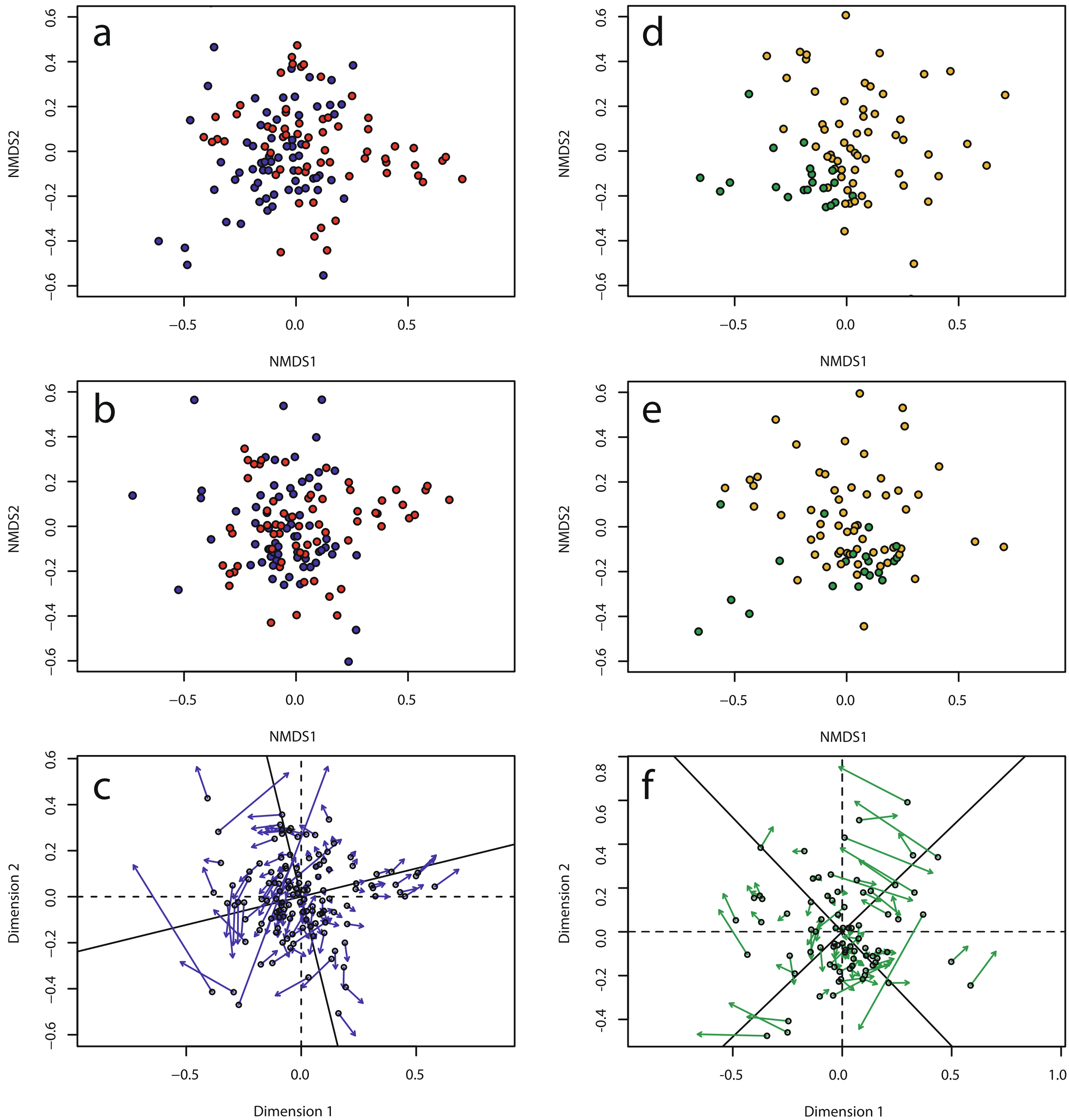

Fig. 7. Plots of the non-metric multidimensional scaling (NMDS) and the Procrustes rotation of site scores on the Danube dataset ($ADMO_{\mathbf{Db}}$; n = 128; 6/a-6/c) and in the $ADMO_{\mathbf{IN}}$ dataset (n = 79; 6/d-6/f). Fig. 7/a. Plot of NMDS scores in the Danubian $ADMO_{Dd\_in}$ dataset (n = 128); red circles represent the samples in which ADMO was present (n = 65) and the blue circles are where ADMO was not present (n = 63). The separation of the two groups is significant (PERMANOVA adonis, F = 12.934 R^2 = 0.0931, p = 0.001). Fig. 7/b. Plot of NMDS scores, after removing ADMO from the Danube dataset; the separation of two groups is also significant (=adonis on NMDS scores (F = 4.4881, R^2 = 0.03439p = 0.015), the colours of groups are the same as in Fig. 7/a). Fig. 7/c. Plot of the residuals from Procrustes analysis for the comparison between the ordinations of $ADMO_{Dd\_in}{}^{+}$ and $ADMO_{Dd\_in}{}^{-}$. Each arrow connects the $ADMO_{Dd\_in}{}^{+}$ and the $ADMO_{Dd\_in}{}^{-}$ count from one site. The arrows point in the direction of the $ADMO_{Dd\_in}{}^{+}$ ordination. The arrow length corresponds to the difference in site location between the two ordinations (correlation = 0.8509, P = 0.001 on 999 permutations). Fig. 7/d. Plot of NMDS scores in the $ADMO_{IN}$ dataset (n = 79); the green circles represent the samples in which ADMO was dominant $ADMO_{IN}{}^{+\geq 5\%}$ while yellow circles show the position of samples in which ADMO was not abundant, $ADMO_{IN}{}^{+<5\%}$. The separation of the two groups is significant (PERMANOVA adonis, F = 19.439, R^2 = 0.20157, p = 0.001). Fig. 7/e Plot of NMDS scores, after removing ADMO from the $ADMO_{IN}$ dataset (green: $ADMO_{IN}{}^{-\geq 5\%}$; yellow: $ADMO_{IN}{}^{-\leq 5\%}$) the separation of the two groups is significant (PERMANOVA adonis, F = 8.7012, R^2 = 0.10153, p = 0.001). Fig. 7/f. Plot of the residuals from Procrustes analysis for the comparison between the ordinations of the $ADMO_{IN}{}^{+}$ and $ADMO_{IN}{}^{-}$ datasets. (For interpretation of the references to colour in this figure legend, the reader is referred to the web version of this article.)

possible that we could reinvestigated the species from samples before 2013, however, no ADMO was found from the middle of 1980th until 2015 in the Hungarian section of the River Danube.

In the present study, ADMO never reached a relative abundance of 5% before 2018 in the River Danube (Trábert et al., 2020, 2017). Since that time, it has proved to be a diatom with a steadily increasing dominance in the phytobenthos of the Danube. Furthermore, it has also begun to appear as a dominant species in the tributaries of the Danube, namely, the Rivers Dráva, Száva and Tisza.

It may reasonably be hypothesized that if elevated temperatures facilitated the spread of ADMO, this diatom would spread from the southern region, the Mediterranean, and would occupy the riverbank from the lower to upper sections of the river (Slynko et al., 2002; Panov et al., 2009). In fact, the dispersion patterns were different; the distribution pattern of ADMO shows a downstream pattern, being found first in the upper section of the Danube, where it became frequent and abundant. Later, its increasing abundance was visible in the middle section of the river, though it remained rare in the lower section. This seems to demonstrate that River Danube is an important invasion route of Europe from North to South and from West to East; the direction of water flow is a main driver for biota of the river (Panov et al., 2009).

The overview of the distribution and dominance of an ‘invisible’ microscopic microorganism is necessarily quite limited, mainly depending on sampling frequency. Only the standard monitoring points can provide information (more or less) about the spread of taxa – always supposing that the identification of taxa is correct. Apart from the large-celled *Didymosphaenia geminata*, most of the invasive diatoms are small, and hardly identifiable. Moreover, a great part of them has only been described recently, due to their small dimensions.

To predict the effects and the directions of the current expansion of the taxon, every single item of data has importance. The present results suggest that ADMO might not only occupy, but also become dominant in further sections of the Danube in the phytobenthic community.

4.3. Environmental variables and associated taxa

The environmental preferences of the species estimated in the present study are mostly in agreement with the previous publications, as ADMO prefers calcareous, eutrophic waters with moderate to high electrolyte content (Pérès et al., 2012; Falasco et al., 2016; Peeters and Ector 2018). The most detailed data of the environmental variables were presented by Pérès et al., (2012), where minimum and maximum values of 26 physico–chemical parameters were given from 11 localities where ADMO was recorded. Altogether 14 variables of them are common and comparable in our dataset and that of Pérès et al. (2012). Usually, the estimated optimum, including their tolerance in our study are in the range presented by Pérès et al. (2012) for 12 variables (as conductivity, pH, dissolved organic material (DO), Temperature (T), Phosphorous forms, Total Phosphorous (TP), nitrogen-nitrate ($N\text{-}NO_3^-$), calcium (Ca^{2+}), natrium (Na^{+}), hydrogen-carbonate (HCO_3^-), sulphate (SO_4^{2-}), chloride (Cl^-).

Only the magnesium and potassium values showed remarkable differences to the results of Pérès et al. (2012). Based on our study the Mg^{2+} optima were higher (opt = 30.2 mg L $^{-1}$ tol = 4.5 mg L $^{-1}$), while only 9.4 mg L $^{-1}$ was indicated as the maximum values in Pérès et al. (2012). The Mg^{2+} content of surface waters is important factor mainly determined by the bedrock of the watercourse. The K^+ values showed the same feature, it was higher in our study than in Pérès et al., (2012) who published, 1.1 mg L^{-1} and 3.7 mg L^{-1} for the two extrema, while according to our estimation it’s optimum was 4.7 mg L^{-1} with 0.4 mg L $^{-1}$ tolerance. The elevated level of potassium can be connection with the changes of land use and wastewater contamination (Skowron et al., 2018).

According to our study, temperature optima of the species was 21.8 °C and the relative abundance of ADMO was higher in samples collected in summer than in spring or autumn. In the recent decades rising water temperature of the River Danube were regularly reported (Duleba et al., 2014; Dokulil, 2014, 2018; Abonyi et al., 2018), which could favour the appearance and proliferation of other non-native diatom species like *Skeletonema potamos* in the phytoplankton (Duleba et al., 2014) and now, may provide increasingly favourable conditions for the spread of ADMO in the phytobenthos. Further observation can support its warmer water preference, as its rapid occupation of the outflow of nuclear power plant (NPP) (Paks) in the middle section of the Danube in Hungary. This special habitat (characterized by heat pollution) was occupied by ADMO probably in 2015. Five years later, ADMO reached a relative abundance of more than 90% at the cooling water outlet. This constant and permanent heat pollution may support the proliferation of ADMO. Falasco et al. (2017) also documented the increasing abundance of ADMO in parallel with the enhancing temperature from spring to autumn, when ADMO dominated the communities, and in some cases, it reached almost 70 % in relative abundance.

As for associated taxa, where ADMO dominated the assemblages (i.e. at relative abundances of at least 5%), most of the co-occurring taxa are eutrophic, β-meso-saprobic, and some are α-meso-saprobic (Van Dam et al., 1994), which is in accordance with the physical and chemical data. *Amphora pediculus*, *Achnanthidium minutissimum*, *Navicula cryptotenella* Lange–Bertalot 1985 were often reported as associated taxa in cases where ADMO was strongly dominant (Pérès et al., 2012). Falasco et al. (2016) described *Achnanthidium minutissimum* as the most abundant and frequent species, followed by *Achnanthidium pyrenaicum* and *Amphora pediculus* in all samples where ADMO was also dominant.

4.4. Site-specific Biological Contamination index and the impact of ADMO to diatom community

The use of Site-specific Biological Contamination (SBC) Index has been a long history in Joint Danube Surveys. It has applied from the outset (2001) of JDS for aquatic macrophytes and macroinvertebrates (JDS1–JDS4) and later (from the JDS2), it was also used for fishes (Csányi et al., 2021; Liska et al., 2021). The SBC Index for macroinvertebrates and fish usually indicated that majority of the sites are highly to severely contaminated by invasive species, and SBC generally increasing in time along the River Danube (Csányi et al., 2021; Liska et al., 2021). SBC Index was applied first time to phytobenthos – as the fourth of the Biological Quality Elements (EQRs) of Water Framework Directives – for estimating the level of diatom invasion in this study. The calculated SBC values (0.01–0.62) indicated well not only the most infected sites but first signs of the occupation of the incomers: strong associated correlation between relative abundance of ADMO and SBC index values is spurious, because SBC highly dependent on the ADMO, as the most abundant AIS. Less, but also significant and positive correlation was found between the logarithmic relative abundance of ADMO and SBC index values calculated without ADMO. We are far from the understanding the functional responses of biota on assemblages’ level to the continuous impacts like invasion (Cuthbert and Briski 2021), but the here presented data may demonstrate that the riverine biofilm is under permanent pressure by different AIS. SBC index proved to be a useful tool for assessing the presence and abundance of invaders in freshwaters. Our results can provide as a SBC reference for detecting the forthcoming changes in diatom invasion and connected ecological status. The results of the present study also demonstrate that the appearance and spread of ADMO made significant changes in diatom community structure of the phytobenthos along the River Danube, similarly to other AIS, which have negative and sometimes irreversible impact on ecosystems (species extinction, decreasing of biodiversity) (Vilà et al., 2011; Poland, 2021).

5. Conclusions

The present study provides the first evidence for the rapid and abrupt spread of *Achnanthidium delmontii,* a tiny monoraphid diatom, along the River Danube. This invader occupied the riverbank and quickly became the dominant benthic species of the river causing the reorganisation of the phytobenthos communities. ADMO prefers higher water temperatures which can draw attention to its potential relationship with global warming, however, its spread shows a downstream pattern; in contrast to the hypothesized route (from the Mediterranean to North Europe) demonstrating that, the River Danube an important invasion corridor of Europe.

Declaration of Competing Interest

The authors declare that they have no known competing financial interests or personal relationships that could have appeared to influence the work reported in this paper.

Acknowledgements

"This product includes data licensed from International Commission for the Protection of the Danube River (ICPDR)." Special thanks go to Marina Ivanković, the visitor of Danube Research Institute in 2016, whose samples collected in the Austrian section of the River Danube in summer 2014 and 2015 drew our attention to *Achnanthidium delmontii* – the first pictures were taken from her samples. We are also grateful to the anonymous reviewers for providing criticisms and helpful suggestions.

This study was supported by the National Research Development and Innovation Office (NKFIH, OTKA 119208 and NKFIH K137950), National Research, Development and Innovation Office (KEHOP-1.1.0-15-2016-0002), Premium Postdoctoral Research Program of the Hungarian Academy of Sciences [PPD2018-026/2018] and Centre for Ecological Research (BA4902/21 Riverine Project)

References

Abonyi, A., Ács, É., Hidas, A., Grigorszky, I., Várbíró, G., Borics, G., Kiss, K.T., 2018. Functional diversity of phytoplankton highlights long-term gradual regime shift in the middle section of the Danube River due to global warming, human impacts and oligotrophication. Freshw. Biol. 63 (5), 456–472. https://doi.org/10.1111/fwb.13084.

Anderson, M.J., Walsh, D.C.I., 2013. PERMANOVA, ANOSIM, and the Mantel test in the face of heterogeneous dispersions: what null hypothesis are you testing? Ecol. Monogr. 83, 557–574. https://doi.org/10.1890/12-2010.1.

Arbačiauskas, K., Semenchenko, V., Grabowski, M., Leuven, R., Paunović, M., Son, M., Csányi, B., Gumuliauskaitė, S., Konopacka, A., Nehring, S., van der Velde, G., Vezhnovetz, V., Panov, V., 2008. Assessment of biocontamination of benthic macroinvertebrate communities in European inland waterways. Aquat. Invasions 3 (2), 211–230. https://doi.org/10.3391/ai.2008.3.2.12.

Blanco, S., Ector, L., 2009. Distribution, ecology and nuisance effects of the freshwater invasive diatom Didymosphenia geminata (Lyngbye) M. Schmidt: a literature reviewDistribution, ecology and nuisance effects of the freshwater invasive diatom Didymosphenia geminata (Lyngbye) M. Schmidt: a literature review. nova_hedwigia. https://doi.org/10.1127/0029-5035/2009/0088-0347.

Borcard, D., Gillet, F., Legendre, P., 2018. Numerical ecology with R. Springer.

Bray, J., Harding, J.S., Kilroy, C., Broady, P., Gerbeaux, P., 2016. Physicochemical predictors of the invasive diatom Didymosphenia geminata at multiple spatial scales in New Zealand rivers. Aquat. Ecol. 50, 1–14. https://doi.org/10.1007/s10452-015-9543-2.

CEN, 2014. EN 13946. Water quality – guidance for the routine sampling and preparation of benthic diatoms from rivers and lakes. European Committee for Standardization, Brussels, Belgium.

Ciugulea, I., Potapova, M., 2021. Achnanthidium delmontii. In Diatoms of North America. [WWW Document]. URL https://diatoms.org/species/achnanthidium-delmontii (accessed 6.21.21).

Clarke, K.R., 1993. Non-parametric multivariate analyses of changes in community structure. Austral Ecol. 18, 117–143. https://doi.org/10.1111/j.1442-9993.1993.tb00438.x.

Coste, M., Ector, L., 2000. Invasive, exotic or rare diatoms in France: main observations during the last decades. Syst. Geogr. Plants 70, 373–400. https://doi.org/10.2307/3668651.

Crossetti, L.O., Bicudo, D.d.C., Bini, L.M., Dala-Corte, R.B., Ferragut, C., de Mattos Bicudo, C.E., 2019. Phytoplankton species interactions and invasion by Ceratium furcoides are influenced by extreme drought and water-hyacinth removal in a shallow tropical reservoir. Hydrobiologia 831, 71–85. https://doi.org/10.1007/s10750-018-3607-y.

Csányi, B., Weiperth, A., Zorić, K., Bammer, V., Borza, P., Trichkova, T., Weigand, A., Cardoso, A.C., Očadlik, M., Bubíková, K., Stanković, I., Teodorov, M., Botev, I., Kenderov, M., Hubenov, Z., Paunović, M., 2021. Chapter 10: Invasive alien species. In: Joint Danube Survey 4 Scientific Report: A Shared Analysis of the Danube River. International Commission for the Protection of the River Danube, Vienna, Austria, pp. 93–106.

Cuthbert, R.N., Briski, E., 2021. Temperature, not salinity, drives impact of an emerging invasive species. Sci. Total Environ. 780, 146640. https://doi.org/10.1016/j.scitotenv.2021.146640.

Dokulil, M., 2018. Climate warming affects water temperature in the River Danube and tributaries–present and future perspectives. Geomorphol. Slovaca Bohem. 18, 57–63.

Dokulil, M., 2014. Impact of climate warming on European inland waters. Inland Waters 4, 27–40. https://doi.org/10.5268/IW-4.1.705.

Duleba, M., Ector, L., Horváth, Z., Kiss, K.T., Molnár, L.F., Pohner, Z., Szilágyi, Z., Tóth, B., Vad, C.F., Várbíró, G., Ács, É., 2014. Biogeography and Phylogenetic Position of a Warm-stenotherm Centric Diatom, Skeletonema potamos (C.I. Weber) Hasle and its Long-term Dynamics in the River Danube. Protist 165, 715–729. https://doi.org/10.1016/j.protis.2014.08.001.

Ector, L., Hlubikova, D., Cejudo Figueiras, C., Hoffmann, L., Blanco Lanza, S., 2017. Rare and exotic diatoms in the Duero River basin (NW Spain), with notes on their ecology and world distribution. Scripta Bot, Belg, p. 45.

Falasco, E., Piano, E., Bona, F., 2016. Diatom flora in Mediterranean streams: flow intermittency threatens endangered species. Biodivers. Conserv. 25, 2965–2986. https://doi.org/10.1007/s10531-016-1213-8.

Fidlerová, D., Makovinská, J., 2021. Chapter 7: Phytobenthos. In: Joint Danube Survey 4 Scientific Report: A Shared Analysis of the Danube River. International Commission for the Protection of the River Danube, Vienna, Austria, pp. 65–72.

Gower, J.C., 1971. A general coefficient of similarity and some of its properties. Biometrics 857–871. https://www.jstor.org/stable/2528823.

Jellyman, P.G., Clearwater, S.J., Clayton, J.S., Kilroy, C., Blair, N., Hickey, C.W., Biggs, B.J.F., 2011. Controlling the Invasive Diatom Didymosphenia geminata: an Ecotoxicity Assessment of Four Potential Biocides. Arch. Environ. Contam. Toxicol. 61, 115–127. https://doi.org/10.1007/s00244-010-9589-z.

Keck, F., Vasselon, V., Rimet, F., Bouchez, A., Kahlert, M., 2018. Boosting DNA metabarcoding for biomonitoring with phylogenetic estimation of operational taxonomic units' ecological profiles. Mol. Ecol. Resour. 18, 1299–1309. https://doi.org/10.1111/1755-0998.12919.

Lange-Bertalot, H., Hofmann, G., Werum, M., Cantonati, M., 2017. Freshwater Benthic Diatoms of Central Europe: Over 800 Common Species Used in Ecological Assessment. Koeltz Botanical Books Schmitten-Oberreifenberg.

Liška, I., Wagner, F., Sengl, M., Deutsch, K., Slobodník, J., Paunović, M., 2021. Joint Danube Survey 4 Scientific Report: A Shared Analysis of the Danube River. Austria, Vienna.

Ludwig, J.A., Reynolds, J.F., 1988. Statistical Ecology: a Primer on Methods & Computing. John Wiley & Sons Inc, USA.

Macêdo, R.L., Russo, P., Corrêa, R.F., Rocha, O., dos Santos, L.N., Branco, C.W.C., 2021. The drifting dinoflagellate Ceratium furcoides (Levander) Langhans 1925: fundamental niche shift during global invasion. Hydrobiologia 848. https://doi.org/10.1007/s10750-020-04495-5.

Martín, G., Toja, J., Sala, S.E., Fernández, M.d.L.R., Reyes, I., Casco, M.A., 2010. Application of diatom biotic indices in the Guadalquivir River Basin, a Mediterranean basin. Which one is the most appropriated? Environ. Monit. Assess. 170, 519–534.

Mather, L., MacIntosh, K., Kaczmarska, I., Klein, G., Martin, J.L., 2010. A checklist of diatom species reported (and presumed native) from Canadian coastal waters. Can Tech Rep Fish Aquat Sci 2881, 1–78.

Miao, M., Li, Z., Hwang, E.-A., Kim, H.-K., Lee, H., Kim, B.-H., 2020. Two New Benthic Diatoms of the Genus Achnanthidium (Bacillariophyceae) from the Hangang River. Korea. Diversity 12, 285. https://doi.org/10.3390/d12070285.

Moreira, R.A., Rocha, O., Santos, R.M., Laudares-Silva, R., Dias, E.S., Eskinazi-Sant'Anna, E.M., 2015. First record of Ceratium furcoides (Dinophyta), an invasive species, in a temporary high-altitude lake in the Iron Quadrangle (MG, Southeast Brazil). Braz. J. Biol. 75 (1), 98–103.

Nistal-García, A., García-García, P., García-Girón, J., Borrego-Ramos, M., Blanco, S., Bécares, E., 2021. DNA metabarcoding and morphological methods show complementary patterns in the metacommunity organization of lentic epiphytic diatoms. Sci. Total Environ. 786, 147410. https://doi.org/10.1016/j.scitotenv.2021.147410.

Novais, M.H., Jüttner, I., Vijver, B.V.D., Morais, M.M., Hoffmann, L., Ector, L., 2015. Morphological variability within the Achnanthidium minutissimum species complex (Bacillariophyta): comparison between the type material of Achnanthes minutissima and related taxa, and new freshwater Achnanthidium species from Portugal. Phytotaxa 224, 101. https://doi.org/10.11646/phytotaxa.224.2.1.

Oksanen, J., Blanchet, F.G., Kindt, R., Legendre, P., Minchin, P.R., O'hara, R.B., Simpson, G.L., Solymos, P., Stevens, M.H.H., Wagner, H., 2013. Package 'vegan.' Community Ecol. Package Version 2, 1–295.

Oksanen, J., Kindt, R., Legendre, P., O'Hara, B., Stevens, M.H.H., Oksanen, M.J., Suggests, M., 2007. The vegan package. Community Ecol. Package 10, 719.

Panov, V.E., Alexandrov, B., Arbačiauskas, K., Binimelis, R., Copp, G.H., Grabowski, M., Lucy, F., Leuven, R.S., Nehring, S., Paunović, M., Semenchenko, V., Son, M.O., 2009. Assessing the risks of aquatic species invasions via european inland waterways: from concepts to environmental indicators. Integr. Environ. Assess. Manag. 5, 110–126. https://doi.org/10.1897/IEAM_2008-034.1.

Paunović, M., Csányi, B., Simonović, P., Zorić, K., 2015. Invasive Alien Species in the Danube, in: Liska, I. (Ed.), The Danube River Basin, The Handbook of Environmental Chemistry. Springer, Berlin, Heidelberg, pp. 389–409. 10.1007/698_2015_376.

Pérès, F., Barthès, A., Ponton, E., Coste, M., Ten-Hage, L., Le-Cohu, R., 2012. Achnanthidium delmontii sp. nov., a new species from French rivers. Fottea 12 (2), 189–198. https://doi.org/10.5507/fot.2012.014.

Peres-Neto, P.R., Jackson, D.A., 2001. How well do multivariate data sets match? The advantages of a Procrustean superimposition approach over the Mantel test. Oecologia 129 (2), 169–178. https://doi.org/10.1007/s004420100720.

Plamen, I.N., 2018. Two new diatom species from family Achnanthidiaceae in Bulgaria: Achnanthidium druartii, an invasive species in Europe and Achnanthidium straubianum, new to Bulgarian diatom flora. Phytol Balc 24, 195–199.

Poland, T.M., 2021. Regional Summaries. Invasive Species For. Rangel. U. S. 335. doi.org/10.1007/978-3-030-45367-1.

Ponader, K.C., Potapova, M.G., 2007. Diatoms from the genus Achnanthidium in flowing waters of the Appalachian Mountains (North America): ecology, distribution and taxonomic notes. Limnologica 37, 227–241. https://doi.org/10.1016/j.limno.2007.01.004.

R Core Team, 2020. R: A language and environment for statistical computing. R Foundation for Statistical Computing, Vienna, Austria.

Peeters, V., Ector, L. 2018. Atlas des diatomées des cours d'eau du territoire bourguignon. Volume 2: Monoraphidées, Brachyraphidées. pp. 271. Direction Bourgogne Régionale de l'Environnement, de l'Aménagement et du Logement Bourgogne-Franche-Comté.

Rimet, F., Bouchez, A., 2012. Life-forms, cell-sizes and ecological guilds of diatoms in European rivers. Knowl. Managt. Aquatic Ecosyst. (406), 01. https://doi.org/10.1051/kmae/2012018.

Rimet, F., Bouchez, A., Tapolczai, K., 2016. Spatial heterogeneity of littoral benthic diatoms in a large lake: monitoring implications. Hydrobiologia 771 (1), 179–193.

Rimet, F., Chonova, T., Gassiole, G., Gusev, E., Kahlert, M., Keck, F., Kelly, M., Kochoska, H., Kulikovskiy, M., Levkov, Z., Maltsev, Y., Mann, D., Pfannkuchen, M., Trobajo, R., Vasselon, V., Wetzel, C., Zimmermann, J., Bouchez, A., 2019. "Diat.barcode, an open-access barcode library for diatoms", 10.15454/TOMBYZ, Portail Data INRAE, V11.

Rimet, F., Couté, A., Piuz, A., Berthon, V., Druart, J.-C., 2010. Achnanthidium druartii sp. nov. (Achnanthales, Bacillariophyta), a new species invading European rivers. Vie MilieuLife Environ. 185–195.

Sastre, A.V., Santinelli, N.H., Bauer, G.A., Ayesterán, M.G., Uyua, N.M., 2013. First record of the invasive diatom Didymosphenia geminata (Lyngbye) Schmidt in a Patagonian Andean river of Argentina. 10.3391/bir.2013.2.1.02.

Skowron, P., Skowrońska, M., Bronowicka-Mielniczuk, U., Filipek, T., Igras, J., Kowalczyk-Juśko, A., Krzepiłko, A., 2018. Anthropogenic sources of potassium in surface water: the case study of the Bystrzyca river catchment, Poland. Agric. Ecosyst. Environ. 265, 454–460. https://doi.org/10.1016/j.agee.2018.07.006.

Slynko, Y.V., Korneva, L.G., Rivier, I.K., Papchenkov, V.G., Scherbina, G.H., Orlova, M.I., Therriault, T.W., 2002. The Caspian-Volga-Baltic invasion corridor. In: Leppäkoski, E., Gollasch, S., Olenin, S. (Eds.), Invasive Aquatic Species of Europe. Distribution, Impacts and Management. Springer Netherlands, Dordrecht, pp. 399–411. https://doi.org/10.1007/978-94-015-9956-6_40.

Spaulding, S.A., Kilroy, C., Edlund, M.B., 2010. Diatoms as non-native species, in: The Diatoms: Applications for the Environmental and Earth Sciences. University Press. 686 p Cambridge, pp. 560–569.

Tapolczai, K., Selmeczy, G.B., Szabó, B., B-Béres, V., Keck, F., Bouchez, A., Rimet, F., Padisák, J., 2021. The potential of exact sequence variants (ESVs) to interpret and assess the impact of agricultural pressure on stream diatom assemblages revealed by DNA metabarcoding. Ecol. Ind. 122, 107322. https://doi.org/10.1016/j.ecolind.2020.107322.

Trábert, Z., Duleba, M., Bíró, T., Dobosy, P., Földi, A., Hidas, A., Kiss, K.T., Óvári, M., Takács, A., Várbíró, G., Záray, G., Ács, É., 2020. Effect of land use on the Benthic Diatom Community of the Danube River in the Region of Budapest. Water 12, 479. https://doi.org/10.3390/w12020479.

Trábert, Z., Tihamér Kiss, K., Várbíró, G., Dobosy, P., Grigorszky, I., Ács, É., 2017. Comparison of the utility of a frequently used diatom index (IPS) and the diatom ecological guilds in the ecological status assessment of large rivers. Fundam. Appl. Limnol. 189 (2), 87–103. https://doi.org/10.1127/fal/2016/0933.

Van Dam, H., Mertens, A., Sinkeldam, J., 1994. A coded checklist and ecological indicator values of freshwater diatoms from The Netherlands. Netherland J. Aquat. Ecol. 28, 117–133. https://doi.org/10.1007/BF02334251.

Vasselon, V., Bouchez, A., Rimet, F., Jacquet, S., Trobajo, R., Corniquel, M., Tapolczai, K., Domaizon, I., Mahon, A., 2018. Avoiding quantification bias in metabarcoding: application of a cell biovolume correction factor in diatom molecular biomonitoring. Methods Ecol. Evol. 9 (4), 1060–1069. https://doi.org/10.1111/2041-210X.12960.

Vasselon, V., Rimet, F., Tapolczai, K., Bouchez, A., 2017. Assessing ecological status with diatoms DNA metabarcoding: Scaling-up on a WFD monitoring network (Mayotte island, France). Ecol. Ind. 82, 1–12. https://doi.org/10.1016/j.ecolind.2017.06.024.

Vilà, M., Espinar, J.L., Hejda, M., Hulme, P.E., Jarošík, V., Maron, J.L., Pergl, J., Schaffner, U., Sun, Y., Pyšek, P., 2011. Ecological impacts of invasive alien plants: a meta-analysis of their effects on species, communities and ecosystems. Ecol. Lett. 14, 702–708. https://doi.org/10.1111/j.1461-0248.2011.01628.x.

Visco, J.A., Apothéloz-Perret-Gentil, L., Cordonier, A., Esling, P., Pillet, L., Pawlowski, J., 2015. Environmental monitoring: inferring the diatom index from next-generation sequencing data. Environ. Sci. Technol. 49 (13), 7597–7605. https://doi.org/10.1021/es506158m.

Zimmermann, J., Mora, D., Tapolczai, K., Proft, S., Chonova, T., Rimet, F., Bouchez, A., Fidlerová, D., Makovinská, J., Weigand, A., 2021. Chapter 15: Metabarcoding of phytobenthos samples. Joint Danube Survey 4 Scientific Report: A Shared Analysis of the Danube River. International Commission for the Protection of the River Danube, Vienna, Austria.